Article

A New Simple Function for Combustion and Cyclic Variation Modeling in Supercharged Spark Ignition Engines

Stefano Beccari *[ID] and Emiliano Pipitone [ID]

Department of Engineering, University of Palermo, Viale delle Scienze Building 8, 90128 Palermo, Italy; emiliano.pipitone@unipa.it
* Correspondence: stefano.beccari@unipa.it

Abstract: Research in the field of Internal Combustion (IC) engines focuses on the drastic reduction of both pollutant and greenhouse gas emissions. A promising alternative to gasoline and diesel fuel is represented by the use of gaseous fuels, above all green hydrogen but also Natural Gas (NG). In previous works, the authors investigated the performance, efficiency, and emissions of a supercharged Spark Ignition (SI) engine fueled with mixtures of gasoline and natural gas; a detailed research involving the combustion process of this kind of fuel mixture has been previously performed and a lot of experimental data have been collected. Combustion modeling is a fundamental tool in the design and optimization process of an IC engine. A simple way to simulate the combustion evolution is to implement a mathematical function that reproduces the mass fraction burned (MFB) profile; the most used for this purpose is the Wiebe function. In a previous work, the authors proposed an innovative mathematical model, the Hill function, that allowed a better interpolation of experimental MFB profiles when compared to the Wiebe function. In the research work presented here, both the traditional Wiebe and the innovative Hill function have been calibrated using experimental MFB profiles obtained from a supercharged SI engine fueled with mixtures of gasoline and natural gas in different proportions; the two calibrated functions have been implemented in a zero-dimensional (0-D) SI engine model and compared in terms of both Indicated Mean Effective Pressure (IMEP) and cyclic pressure variation prediction reliability. It was found that the Hill function allows a better IMEP prediction for all the operating conditions tested (several engine speeds, supercharging pressures, and fuel mixtures), with a maximum prediction error of 2.7% compared to 4.3% of the Wiebe function. A further analysis was also performed regarding the cyclic pressure variation that affects all the IC engines during combustion and may lead to irregular engine operation; in this case, the Hill function proved to better predict the cyclic pressure variation with respect to the Wiebe function.

Keywords: internal combustion engine; combustion modeling; cyclic variation; natural gas

1. Introduction

One of the greatest challenges of modern IC engine research is the drastic reduction of both pollutant and greenhouse gasses emissions to decrease the urban area's air pollution and mitigate global warming. This ambitious goal requires a transition phase in which the traditional fossil fuels must be gradually replaced by renewable fuels such as, for example, biofuels (bioethanol, biodiesel, etc.) or green hydrogen (produced by renewable resources). During this transition phase, the current engine's fuel economy must be improved and its pollutant emissions must be reduced. The modern passenger cars are often equipped with supercharged down-sized Spark Ignition (SI) engines endowed with direct injection systems [1–6]. Feeding an SI engine with gaseous fuels instead of gasoline is an effective way to reduce pollutant emissions and improve engine efficiency. For this purpose, both liquefied petroleum gas (LPG) and natural gas (NG) can be successfully employed. The authors, in previous research, experimented with the simultaneous combustion of gasoline and gaseous fuel (Double-Fuel combustion, DF) with both a naturally aspirated SI

engine [7,8] and a supercharged one [9]; the authors experimented with a great increase in engine efficiency with a significant reduction of pollutant emissions, compared to the traditional gasoline mode, and the engine performance did not change significantly. The same authors in [10] performed an experimental combustion analysis on the supercharged DF engine and highlighted the effects of engine speed, charging pressure, and NG content in the fuel mixture on the combustion speed. The authors concluded that both supercharging pressure and gasoline content in the fuel mixture produces a combustion speed increase that, in turn, improves the engine efficiency. This wide research activity required sampling a great number of experimental pressure cycles; a portion of these data has been used in subsequent work [11] to calibrate an innovative non-predictive combustion sub-model that, once implemented in a 0-D engine simulation model, proved to predict the NG fueled engine IMEP accurately.

Computer simulations, in particular 0-D and 1-D thermodynamic models, are fundamental tools in the design and optimization process of IC engines [12–14]. All the processes involved in engine operation can be simulated: the flow-through inlet and outlet ducts, the combustion process, the heat transferred to the combustion chamber walls, and many others. Combustion is the process that mostly influences, with its development through the combustion chamber, both engine performance and pollutant emissions [15]. The combustion evolution depends on many factors: in-cylinder pressure and temperature, air/fuel ratio, turbulence intensity, fuel properties, etc. Hence the combustion process is the most difficult to simulate due to its complexity. A wide variety of combustion models have been proposed in the literature for 0-D and 1-D thermodynamic simulations, from the most complex and accurate predictive models, which require great computational efforts and allow reliable prediction of the performance attainable by the engine, to the simpler and easy to implement non-predictive models often employed for rough evaluations. The "two zones" combustion models [16–18] belong to the first category and mostly refer to SI engines: in these models, the mass inside the combustion chamber is divided into burnt and unburnt gases, and the development of the flame front is modeled by evaluating the laminar and turbulent burning speed; this kind of models, after a proper calibration with experimental data, can predict the combustion evolution, and hence the engine performances, in different operating conditions (engine speed, load, air/fuel ratio, etc.). An easier but less accurate way to simulate the combustion evolution is to model the MFB profile using a mathematical function; the most used for this purpose is the well-known Wiebe function [19,20] reported in Equation (1), which shows the typical sigmoidal trend of the experimental MFB profile as a function of crank angle. A double-Wiebe function can be used to simulate compression ignition engine combustion [21] and other kinds of combustions such as HCCI [21,22] (homogeneous charge compression ignition), dual-fuel combustion [21] (diesel-Natural Gas), or gasoline-ethanol fuel blend combustion [23]. As already mentioned, this method is not predictive because the pressure and temperature conditions of the gas are not taken into account, as well as all the other parameters affecting the flame front propagation (turbulence level, air-fuel ratio, residual gas dilution, etc.): once calibrated using experimental data, a single mathematical MFB profile is usually employed for all the engine operating conditions and then it will provide less accurate results compared to the previously described predictive methods.

The following Equation (1) reports the Wiebe function:

$$x_{bw} = 1 - exp\left[-a\left(\frac{\vartheta - \vartheta_0}{\Delta\vartheta}\right)^{m+1}\right] \tag{1}$$

where x_{bw} is the mass fraction burned (MFB) according to the Wiebe function, ϑ is the generic crank angle (CA) (after ignition), ϑ_0 is the spark ignition CA (the start of combustion), $\Delta\vartheta$ is the combustion duration (expressed in Crank Angle Degrees, CAD), a and m are the calibrating coefficients.

In Ref. [11], the authors presented an innovative MFB interpolation function that proved to perform better than the Wiebe function in IMEP prediction. The innovative function is the Hill function that is reported here:

$$x_{bh} = \frac{(\vartheta - \vartheta_0)^n}{(\vartheta_{50} - \vartheta_0)^n + (\vartheta - \vartheta_0)^n}$$

where x_{bh} is the MFB according to the Hill function, ϑ_{50} is the CA corresponding to 50% of the MFB (i.e., $x_b = 50\%$), $(\vartheta_{50} - \vartheta_0)$ and n are the calibrating coefficients; to simplify, it can be set $\delta = (\vartheta_{50} - \vartheta_0)$ and the equation becomes:

$$x_{bh} = \frac{(\vartheta - \vartheta_0)^n}{\delta^n + (\vartheta - \vartheta_0)^n} \tag{2}$$

In Ref. [11], both Hill and Wiebe equations were calibrated using experimental MFB curves and then implemented in a 0-D engine simulation model used to predict the IMEP of a supercharged NG fueled SI engine. The Hill function better interpolates the experimental MFB curves compared to the Wiebe function when the MFB derivative is non-symmetric due to a non-centered spark plug position [11]. Figure 1a shows an experimental MFB curve (and its derivative) interpolated with the best matching Hill and Wiebe functions; it is evident the higher interpolation accuracy of the Hill function that leads to a better pressure curve simulation, as is shown in Figure 1b, and in turn a better IMEP prediction [11].
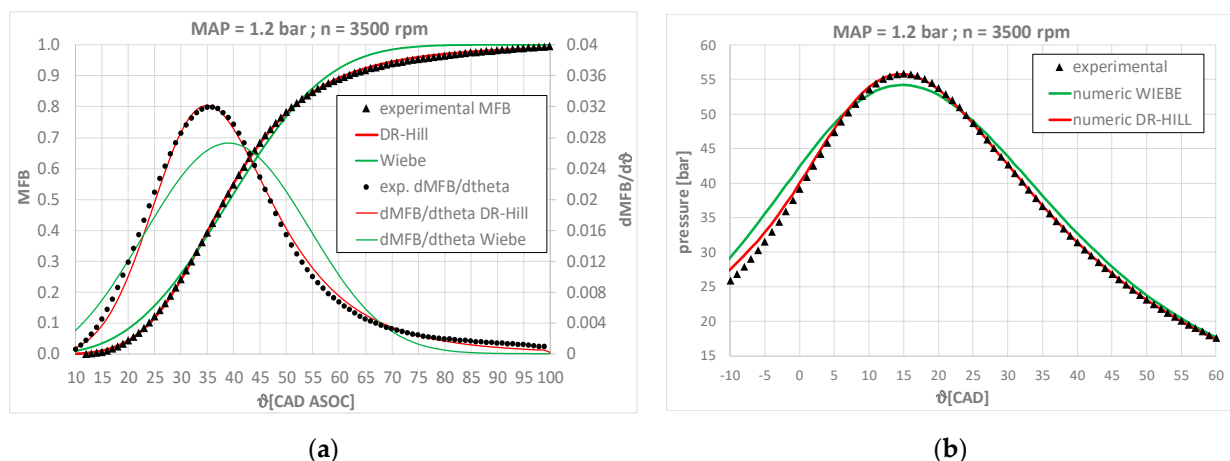

(a)

(b)

Figure 1. 100% NG; MAP = 1.2 bar; *n* = 3500 rpm. (**a**) Experimental MFB profile and its derivative interpolated with the best matching Wiebe and Hill functions; (**b**) Experimental and numeric pressure curves, simulated with the best matching Wiebe and Hill functions.

In the present work, the innovative combustion sub-model (the Hill function) has been calibrated with the complete set of experimental data collected using the DF supercharged engine [9] (i.e., all the DF fuel mixtures have been employed, and not only the pure NG data used in [11]) to predict IMEP in all the engine operating conditions: engine speed, supercharging pressure and fuel mixture composition. Hence this study aims to obtain a wider applicability of the Hill function.

Another important issue concerning the IC engine's operation is the cyclic pressure variation during combustion [24]. It is well known that the pressure evolution in a SI engine always changes from one cycle to another because the phenomena influencing both combustion start and its evolution undergo small stochastic variations. This variability of the cycle pressure produces, in turn, an IMEP variability and may also cause a rough engine operation. The reduction of combustion pressure cyclic variation could improve the engine operation not only in terms of operating smoothness but also in terms of pollutant emissions and knocking resistance. With respect to the nominal combustion phasing

imposed by spark advance, there is a certain amount of pressure cycles that are retarded due to cyclic variation; if the nominal combustion phasing itself is retarded, this may lead, particularly in highly diluted conditions, to poor and incomplete combustions and, in turn, to hydrocarbon emissions. On the other hand, in the case of early combustion phasing, a small number of pressure cycles anticipated with respect to the nominal phasing may lead to knocking. Hence the pressure cyclic variation is a phenomenon that must be accurately studied and taken into account by comprehensive engine models [24].

In the present research, the engine cycle-by-cycle pressure variation has been evaluated and effectively simulated using both the innovative combustion model (the Hill function) and the traditional Wiebe function.

2. Materials and Methods

In the first section of this paper, the two MFB equations (Wiebe and Hill) will be compared in terms of IMEP prediction capabilities based on experimental pressure cycles previously sampled [9] on a supercharged SI engine (whose characteristics are reported in Table 1) fueled with three different mixtures of gasoline and NG; for each fuel mixture, four different charging pressures and eight engine speeds have been tested reaching a total of 96 operating conditions, as reported in Table 2; the fuel mixture has been identified by the mass percentage of NG contained; 100% NG is not present because those results have been already shown in [11]. The setup and procedure used to obtain the experimental MFB curves from the mentioned operating conditions have been widely described in [9,10].

Table 1. Engine technical features.

Engine Specification	Value
Number of intake valves per cylinder	1
Number of exhaust valves per cylinder	1
Cylinders	4
Stroke	78.86 (mm)
Bore	70.8 (mm)
Rod/crank ratio	3.27
Compression ratio	9.8
Engine displacement	1242 (cm^3)
Gasoline port fuel injector	Bosch, model EV6
Natural Gas port fuel injector	Bosch, model EV1

Table 2. Operating conditions tested.

Operating Condition	Value
Manifold air temperature	28 ± 10 (°C)
Manifold Absolute Pressure	1 bar, 1.2 bar, 1.4 bar, 1.6 bar
Speed of the engine	1500, 2000, 2500, 3000, 3500, 4000, 4500, 5000 (rpm)
Spark advance	maximum brake torque value
fuel to air ratio	Stoichiometric
Natural Gas ratio in the fuel mixture	80%, 60%, 40%

For each of the 96 operating conditions reported in Table 2, the experimental MFB curve was used to calibrate both the Wiebe and Hill functions by minimizing the root mean square error (RMSE) between experimental and numerical values; the result is a set of calibration coefficients for each operating condition; as these are not predictive models, a unique value for each calibrating coefficient must be employed for all the engine operating conditions; to this purpose, an average value of the calibrating coefficients has been evaluated for each fuel mixture, as reported in Table 3 (the values of the calibration coefficients obtained in [11] for 100% NG are also reported for comparison).

Table 3. Average calibration coefficients for all the fuel mixtures.

Fuel Mixture	*a* (Wiebe)	*m* (Wiebe)	*δ* (Hill)	*n* (Hill)
40% NG	22.6	2.40	35.8	4.86
60% NG	23.1	2.38	36.3	4.80
80% NG	20.3	2.30	35.7	4.69
100% NG	19.0	2.31	36.9	4.78

The calibrated Wiebe and Hill functions have been hence implemented in a 0-D thermodynamic simulation model (whose detailed description is reported in [11]) used to predict the pressure cycle (and hence the engine IMEP) of the supercharged SI engine fueled with the three different mixtures.

3. Results and Discussion

This section shows the results of the comparison between Hill and Wiebe functions in terms of IMEP and pressure cyclic variation prediction; first of all, the IMEP comparison will be shown.

3.1. IMEP Prediction

Figures 2a,b and 3a,b show the comparison, for the fuel mixture 40% NG and for different supercharging pressures, between the experimental IMEP and the values simulated using both Wiebe and Hill functions together with the histograms of absolute prediction error %. Tables 4–7 show all the numerical IMEP values together with the prediction errors (fuel mixture 40% NG); it is evident the better prediction capability of the Hill function (in particular at MAP 1.4 bar) with an overall average prediction error between 1% and 2.2% compared to Wiebe function that produces an average prediction error between 1.8% and 2.9%.
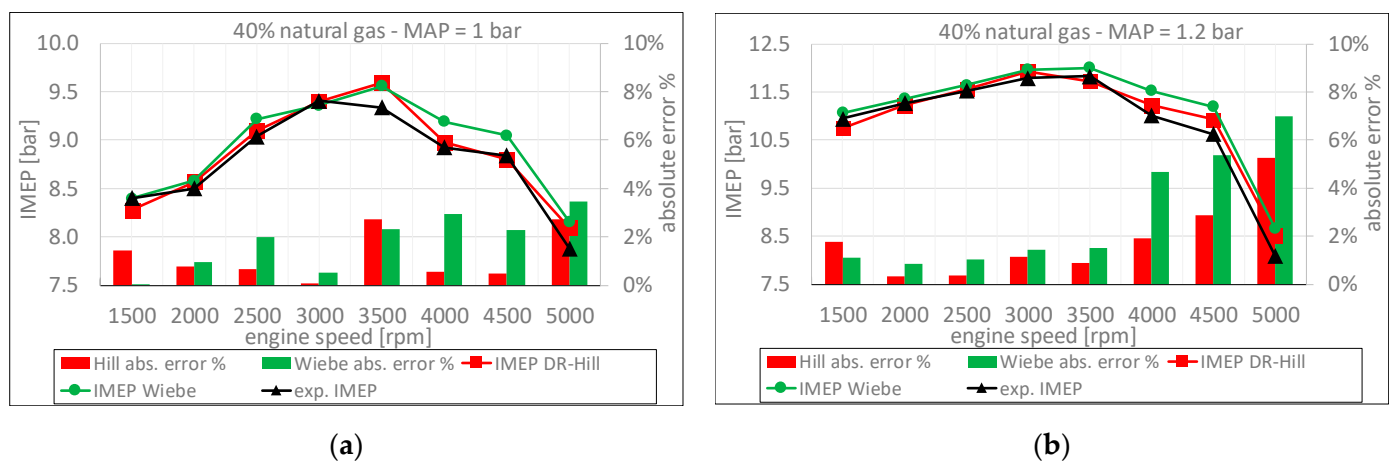

(**a**)

(**b**)

Figure 2. Comparison between the experimental and simulated IMEP; 40% NG fuel mixture. (**a**) MAP = 1 bar. (**b**) MAP = 1.2 bar.
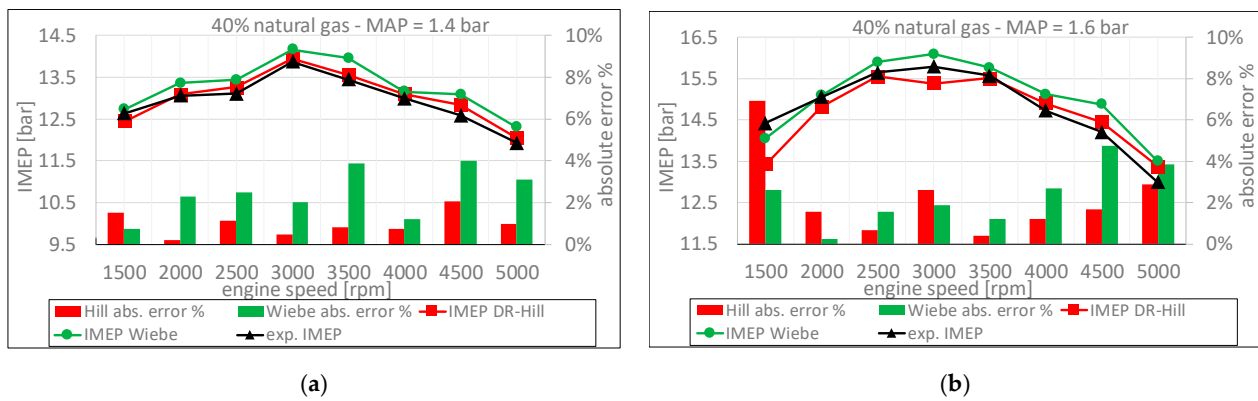
Figure 3. Comparison between the experimental and simulated IMEP; 40% NG fuel mixture. (**a**) MAP = 1.4 bar; (**b**) MAP = 1.6 bar.

Table 4. Experimental and simulated IMEP with absolute prediction errors (40% NG; MAP = 1 bar).

Engine Speed [rpm]	Spark Advance [CAD BTDC]	Engine IMEP [bar]	Hill IMEP [bar]	Wiebe IMEP [bar]	Hill abs. Error %	Wiebe abs. Error %
1500	20	8.399	8.277	8.396	1.5	0.0
2000	24	8.500	8.567	8.581	0.8	1.0
2500	27	9.037	9.097	9.218	0.7	2.0
3000	28	9.408	9.401	9.360	0.1	0.5
3500	29	9.338	9.593	9.556	2.7	2.3
4000	26	8.925	8.974	9.189	0.5	3.0
4500	26	8.843	8.800	9.046	0.5	2.3
5000	25	7.883	8.099	8.156	2.7	3.5
				mean value	**1.2**	**1.8**

Table 5. Experimental and simulated IMEP with absolute prediction errors (40% NG; MAP = 1.2 bar).

Engine Speed [rpm]	Spark Advance [CAD BTDC]	Engine IMEP [bar]	Hill IMEP [bar]	Wiebe IMEP [bar]	Hill abs. Error %	Wiebe abs. Error %
1500	15	10.942	10.749	11.064	1.8	1.1
2000	20	11.262	11.223	11.356	0.3	0.8
2500	20	11.521	11.563	11.640	0.4	1.0
3000	23	11.789	11.926	11.960	1.2	1.5
3500	24	11.824	11.721	12.002	0.9	1.5
4000	23	11.007	11.219	11.523	1.9	4.7
4500	23	10.624	10.928	11.195	2.9	5.4
5000	19	8.088	8.513	8.654	5.3	7.0
				mean value	**1.8**	**2.9**

Table 6. Experimental and simulated IMEP with absolute prediction errors (40% NG; MAP = 1.4 bar).

Engine Speed [rpm]	Spark Advance [CAD BTDC]	Engine IMEP [bar]	Hill IMEP [bar]	Wiebe IMEP [bar]	Hill abs. Error %	Wiebe abs. Error %
1500	16	12.637	12.447	12.731	1.5	0.7
2000	17	13.064	13.093	13.364	0.2	2.3
2500	15	13.114	13.262	13.442	1.1	2.5
3000	17	13.879	13.945	14.162	0.5	2.0
3500	20	13.445	13.558	13.965	0.8	3.9
4000	22	12.999	13.097	13.158	0.8	1.2
4500	21	12.587	12.849	13.090	2.1	4.0
5000	23	11.930	12.046	12.303	1.0	3.1
				mean value	**1.0**	**2.5**

Table 7. Experimental and simulated IMEP with absolute prediction errors (40% NG; MAP = 1.6 bar).

Engine Speed [rpm]	Spark Advance [CAD BTDC]	Engine IMEP [bar]	Hill IMEP [bar]	Wiebe IMEP [bar]	Hill abs. Error %	Wiebe abs. Error %
1500	11	14.428	13.427	14.052	6.9	2.6
2000	12	15.056	14.820	15.093	1.6	0.2
2500	15	15.654	15.551	15.897	0.7	1.6
3000	14	15.799	15.386	16.099	2.6	1.9
3500	17	15.571	15.510	15.762	0.4	1.2
4000	18	14.723	14.902	15.122	1.2	2.7
4500	19	14.211	14.452	14.887	1.7	4.8
5000	19	13.003	13.380	13.506	2.9	3.9
				mean value	**2.2**	**2.4**

In the following Figures 4a,b and 5a,b, the results of the comparison between experimental and simulated IMEP are shown for the fuel mixture 60% NG.
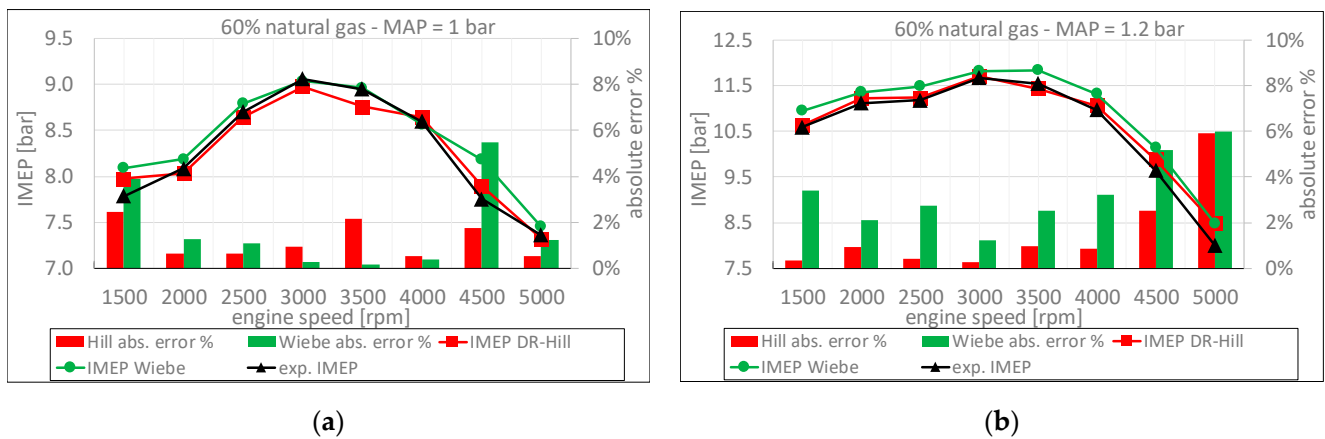

(**a**)　　　　　　　　　　　　　　　　　　　　　　　　(**b**)

Figure 4. Comparison between the experimental and simulated IMEP; 60% NG fuel mixture. (**a**) MAP = 1 bar; (**b**) MAP = 1.2 bar.
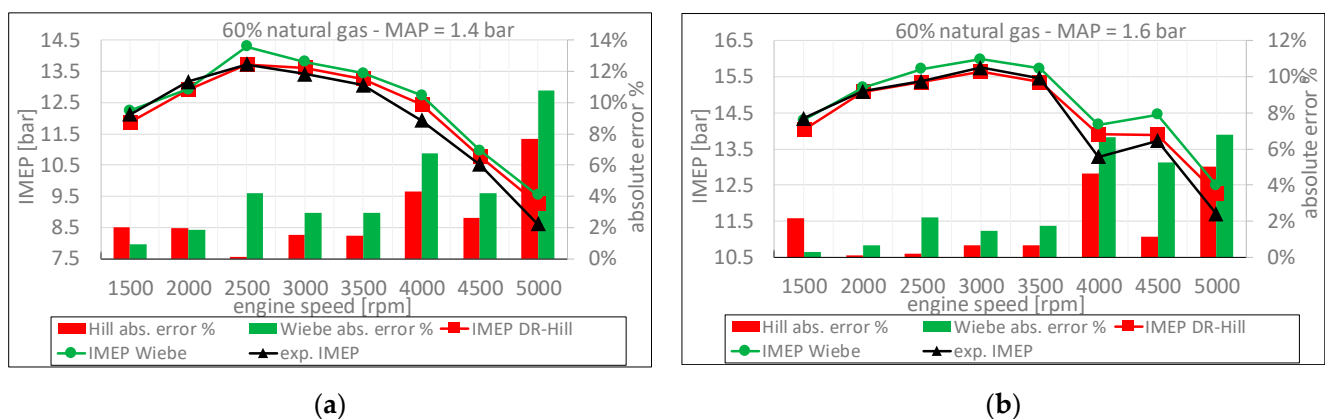

(**a**)　　　　　　　　　　　　　　　　　　　　　　　　(**b**)

Figure 5. Comparison between the experimental and simulated IMEP; 60% NG fuel mixture. (**a**) MAP = 1.4 bar; (**b**) MAP = 1.6 bar.

Tables 8–11 show, for the 60% NG fuel mixture, the numerical values of the IMEP and the absolute prediction error % of the two models (Wiebe and Hill). Once again, it is clear the better prediction capability of the Hill function (in particular at MAP 1.2 and 1.4 bar) with an overall average prediction error between 1.2% and 2.7% compared to the Wiebe function that, produces an average prediction error between 1.7% and 4.3%.

Table 8. Experimental and simulated IMEP with absolute prediction errors (60% NG; MAP = 1 bar).

Engine Speed [rpm]	Spark Advance [CAD BTDC]	Engine IMEP [bar]	Hill IMEP [bar]	Wiebe IMEP [bar]	Hill abs. Error %	Wiebe abs. Error %
1500	24	7.785	7.977	8.089	2.5	3.9
2000	28	8.086	8.033	8.187	0.7	1.2
2500	28	8.702	8.645	8.795	0.7	1.1
3000	28	9.063	8.979	9.040	0.9	0.3
3500	30	8.951	8.759	8.965	2.1	0.2
4000	27	8.600	8.644	8.566	0.5	0.4
4500	22	7.755	7.890	8.181	1.7	5.5
5000	29	7.361	7.321	7.452	0.5	1.2
				mean value	**1.2**	**1.7**

Table 9. Experimental and simulated IMEP with absolute prediction errors (60% NG; MAP = 1.2 bar).

Engine Speed [rpm]	Spark Advance [CAD BTDC]	Engine IMEP [bar]	Hill IMEP [bar]	Wiebe IMEP [bar]	Hill abs. Error %	Wiebe abs. Error %
1500	21	10.592	10.628	10.954	0.3	3.4
2000	23	11.124	11.228	11.359	0.9	2.1
2500	25	11.191	11.238	11.496	0.4	2.7
3000	26	11.678	11.709	11.821	0.3	1.2
3500	27	11.549	11.436	11.842	1.0	2.5
4000	26	10.976	11.068	11.329	0.8	3.2
4500	23	9.639	9.881	10.139	2.5	5.2
5000	22	8.004	8.479	8.485	5.9	6.0
				mean value	**1.5**	**3.3**

Table 10. Experimental and simulated IMEP with absolute prediction errors (60% NG; MAP = 1.4 bar).

Engine Speed [rpm]	Spark Advance [CAD BTDC]	Engine IMEP [bar]	Hill IMEP [bar]	Wiebe IMEP [bar]	Hill abs. Error %	Wiebe abs. Error %
1500	20	12.128	11.883	12.242	2.0	0.9
2000	20	13.167	12.912	12.924	1.9	1.8
2500	20	13.722	13.734	14.294	0.1	4.2
3000	21	13.418	13.620	13.815	1.5	3.0
3500	23	13.066	13.262	13.448	1.5	2.9
4000	20	11.935	12.448	12.739	4.3	6.7
4500	22	10.519	10.793	10.962	2.6	4.2
5000	20	8.605	9.265	9.534	7.7	10.8
				mean value	**2.7**	**4.3**

Table 11. Experimental and simulated IMEP with absolute prediction errors (60% NG; MAP = 1.6 bar).

Engine Speed [rpm]	Spark Advance [CAD BTDC]	Engine IMEP [bar]	Hill IMEP [bar]	Wiebe IMEP [bar]	Hill abs. Error %	Wiebe abs. Error %
1500	16	14.344	14.037	14.304	2.1	0.3
2000	19	15.099	15.087	15.199	0.1	0.7
2500	20	15.383	15.350	15.720	0.2	2.2
3000	19	15.759	15.652	15.987	0.7	1.4
3500	21	15.459	15.355	15.730	0.7	1.8
4000	18	13.288	13.906	14.175	4.7	6.7
4500	23	13.733	13.889	14.454	1.1	5.3
5000	20	11.689	12.274	12.483	5.0	6.8
				mean value	**1.8**	**3.1**

To conclude this comparison, the results of the 80% NG fuel mixture will be shown. In Figures 6a,b and 7a,b, the IMEP comparison for different engine speeds and MAP is presented.
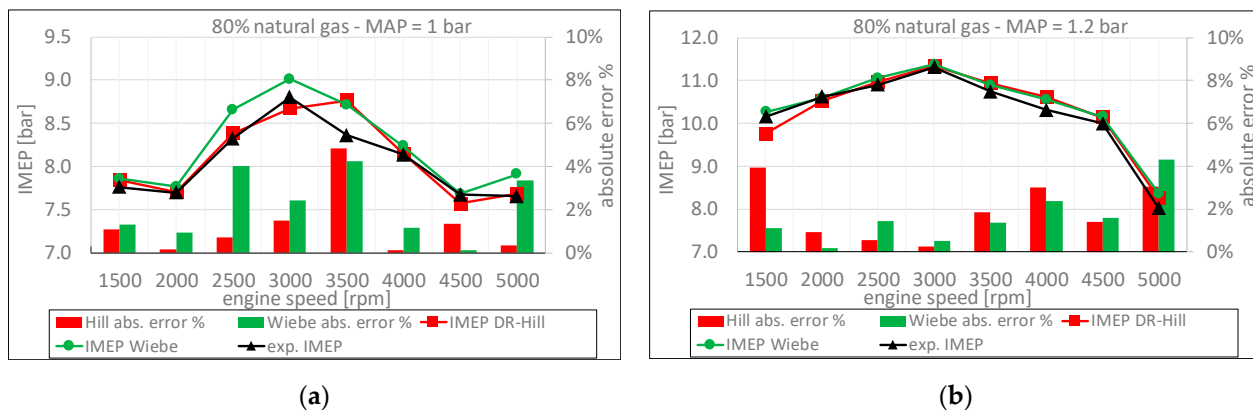

Figure 6. Comparison between the experimental and simulated IMEP; 80% NG fuel mixture. (**a**) MAP = 1 bar; (**b**) MAP = 1.2 bar.
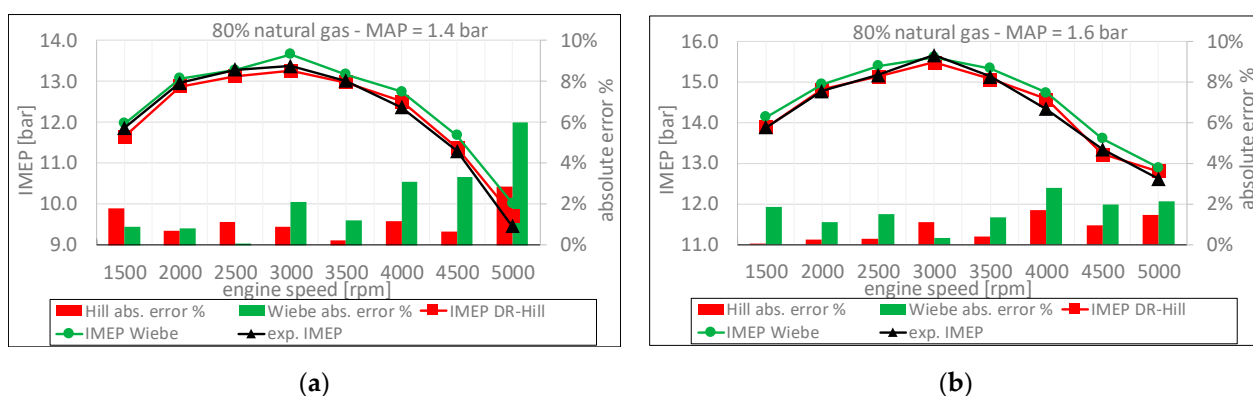

Figure 7. Comparison between the experimental and simulated IMEP; 80% NG fuel mixture. (**a**) MAP = 1.4 bar; (**b**) MAP = 1.6 bar.

In Tables 12–15, the numerical values of IMEP and absolute prediction error % of the two models are reported. Moreover, in this case, the Hill function proved to better predict IMEP values with an average prediction error between 0.8% and 1.9% compared to the Wiebe function, which produces an average prediction error between 1.6% and 2.2%; in this case, the prediction errors of the two models are quite similar.

Table 12. Experimental and simulated IMEP with absolute prediction errors (80% NG; MAP = 1 bar).

Engine Speed [rpm]	Spark Advance [CAD BTDC]	Engine IMEP [bar]	Hill IMEP [bar]	Wiebe IMEP [bar]	Hill abs. Error %	Wiebe abs. Error %
1500	21	7.760	7.843	7.861	1.1	1.3
2000	26	7.694	7.705	7.765	0.1	0.9
2500	26	8.324	8.384	8.659	0.7	4.0
3000	26	8.800	8.670	9.012	1.5	2.4
3500	27	8.360	8.764	8.714	4.8	4.2
4000	26	8.139	8.147	8.234	0.1	1.2
4500	26	7.672	7.569	7.680	1.3	0.1
5000	26	7.655	7.680	7.911	0.3	3.3
				mean value	**1.3**	**2.2**

Table 13. Experimental and simulated IMEP with absolute prediction errors (80% NG; MAP = 1.2 bar).

Engine Speed [rpm]	Spark Advance [CAD BTDC]	Engine IMEP [bar]	Hill IMEP [bar]	Wiebe IMEP [bar]	Hill abs. Error %	Wiebe abs. Error %
1500	19	10.157	9.758	10.269	3.9	1.1
2000	20	10.618	10.519	10.597	0.9	0.2
2500	24	10.905	10.967	11.064	0.6	1.5
3000	23	11.312	11.343	11.371	0.3	0.5
3500	25	10.742	10.943	10.888	1.9	1.4
4000	28	10.313	10.625	10.557	3.0	2.4
4500	28	9.998	10.139	10.158	1.4	1.6
5000	27	8.016	8.261	8.362	3.1	4.3
				mean value	**1.9**	**1.6**

Table 14. Experimental and simulated IMEP with absolute prediction errors (80% NG; MAP = 1.4 bar).

Engine Speed [rpm]	Spark Advance [CAD BTDC]	Engine IMEP [bar]	Hill IMEP [bar]	Wiebe IMEP [bar]	Hill abs. Error %	Wiebe abs. Error %
1500	20	11.860	11.648	11.966	1.8	0.9
2000	21	12.959	12.869	13.065	0.7	0.8
2500	22	13.281	13.130	13.272	1.1	0.1
3000	22	13.375	13.255	13.656	0.9	2.1
3500	23	13.005	12.974	13.165	0.2	1.2
4000	26	12.363	12.506	12.743	1.2	3.1
4500	25	11.299	11.375	11.675	0.7	3.3
5000	23	9.459	9.730	10.026	2.9	6.0
				mean value	**1.2**	**2.2**

Table 15. Experimental and simulated IMEP with absolute prediction errors (80% NG; MAP = 1.6 bar).

Engine Speed [rpm]	Spark Advance [CAD BTDC]	engine IMEP [bar]	Hill IMEP [bar]	Wiebe IMEP [bar]	Hill abs. Error %	Wiebe abs. Error %
1500	20	13.886	13.884	14.144	0.0	1.9
2000	20	14.782	14.819	14.946	0.3	1.1
2500	22	15.172	15.132	15.397	0.3	1.5
3000	22	15.660	15.487	15.610	1.1	0.3
3500	24	15.133	15.076	15.338	0.4	1.4
4000	25	14.340	14.585	14.741	1.7	2.8
4500	26	13.348	13.224	13.609	0.9	2.0
5000	27	12.621	12.804	12.891	1.4	2.1
				mean value	**0.8**	**1.6**

Considering all the operative conditions tested, the average prediction error (indicated as "mean value" in the previous tables) using the Hill function goes from 0.8% to 2.7%, while using the Wiebe function, it goes from 1.6% to 4.3%. To conclude, it can be stated that the Hill function allows to predict the engine IMEP with a greater precision, with respect to the Wiebe function, in a wide range of engine speed, MAP, and fuel mixtures, and this extends the use of Hill function to the simulation of gasoline and gas-fueled SI engines, both in naturally aspirated and supercharged operation.

3.2. Cyclic Variation Prediction

The combustion pressure cyclic variation afflicts all the IC engines and also the SI engine, which is the subject of the present research. The combustion evolution is influenced by some physical phenomena that undergo stochastic variations and, in turn, produce a variability of pressure evolution: the combustion start does not always correspond with the imposed spark advance; the duration of the first part of combustion, characterized by a low burning speed, can vary according to the thermodynamic conditions, the local

dilution and the turbulence inside the combustion chamber; the rapid combustion phase is influenced by pressure and temperature as well as by turbulence levels and the combustion extinction phase is influenced by the flame front cooling due to the chamber walls approach. A possible way to predict the pressure cyclic variation is to study in detail the variation of the above-mentioned phenomena [24]; this approach requires predictive combustion sub-models, such as the two-zones model, which are computationally expensive. The different approach proposed here, which is applicable when the combustion is modeled using a non-predictive method such as Wiebe or Hill functions, is to impose a stochastic variation of the calibration coefficients of such equations to obtain different MFB curves and, in turn, different pressure evolutions. First of all, the experimental pressure cyclic variation must be evaluated and quantified using a proper indicator. As far as the engine IMEP is calculated using a pressure cycle obtained by averaging a certain number of acquired cycles, a preliminary step is to decide how many pressure cycles need to be acquired in a fixed operating condition to obtain a statistically significant population. Figure 8a,b show the result of 500 consecutive pressure cycles acquisition and the corresponding distribution of calculated IMEP (one for each cycle): it is evident, in (b), an almost Gaussian trend, and this implies that its standard deviation (SD) can be adopted as the cyclic variation indicator.

(**a**) 500 consecutive pressure cycles

(**b**) histogram of IMEP distribution
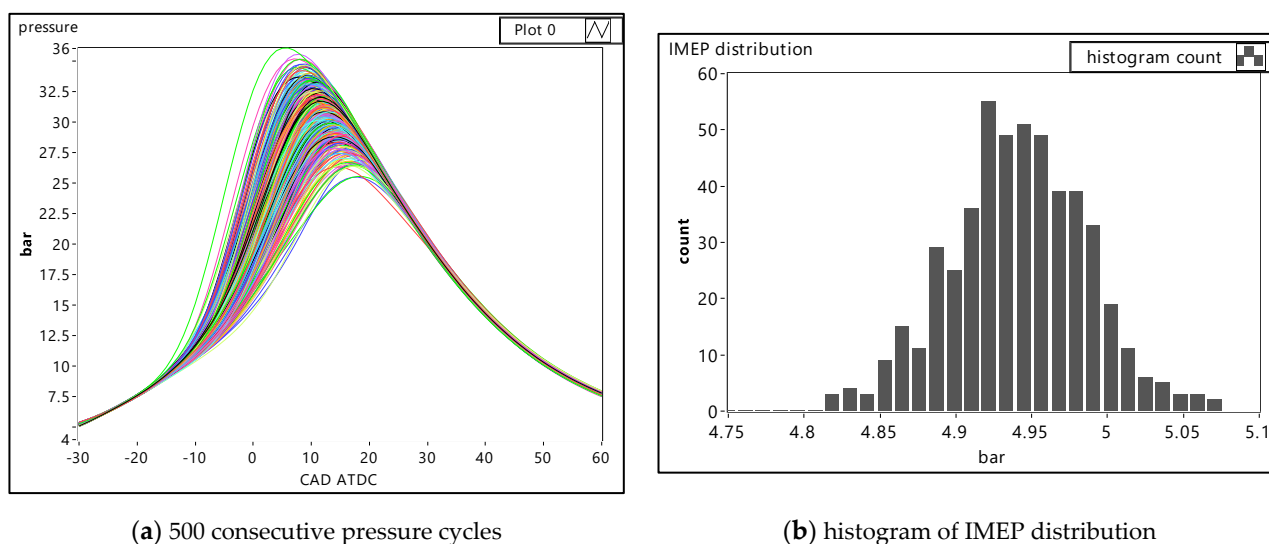
Figure 8. MAP = 0.5 bar, engine speed *n* = 3000 rpm.

In Figure 9a, the diagram reports the average IMEP (i.e., evaluated based on the average pressure cycle) as a function of the number of pressure cycles considered for calculation; the same diagram also shows the absolute percentage IMEP difference with respect to the one evaluated considering all 500 cycles, that is set as a benchmark; the same evaluations were repeated for the IMEP standard deviation and are reported in Figure 9b.

From the analysis of the two diagrams, it can be noted that when the average IMEP and its SD are evaluated with more than 100 pressure cycles, the difference with respect to the benchmark (500 cycles) falls below acceptable levels. The authors concluded hence that, for each operating condition, the acquisition of 100 pressure cycles is a good compromise between obtaining a significant population and reducing the amount of data to handle.

Figure 10a shows 100 consecutive pressure cycles acquired from the SI engine of Table 1 working in a fixed operating condition (100% NG, MAP = 1 bar, engine speed *n* = 3500 rpm) and Figure 10b shows the corresponding histogram of IMEP distribution (mean IMEP = 9.11 bar and SD = 0.214 bar).
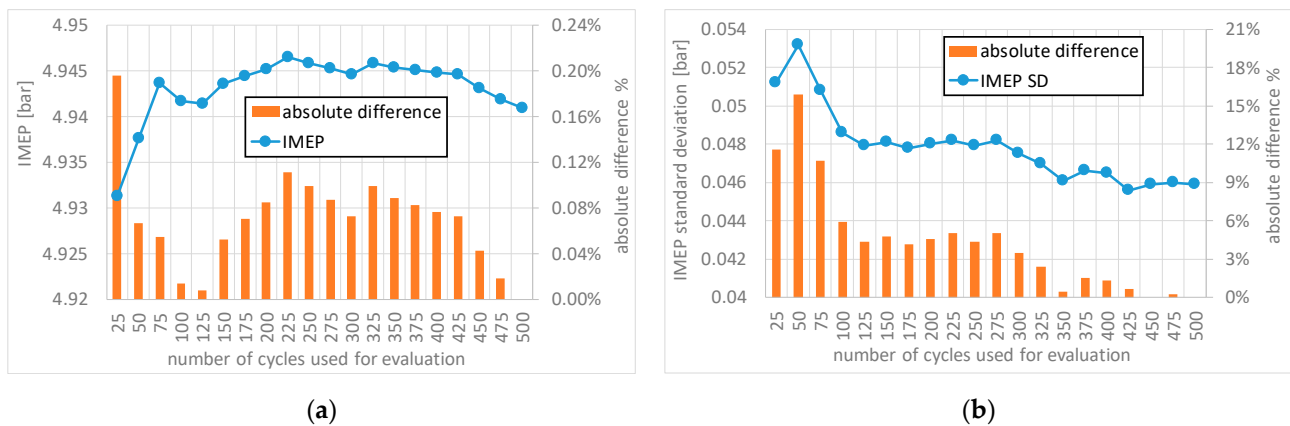
(**a**)

(**b**)

Figure 9. MAP = 0.5 bar, engine speed *n* = 3000 rpm. (**a**) average IMEP and absolute difference% vs. number of cycles taken for evaluation; (**b**) IMEP SD and absolute difference% vs. number of cycles taken for evaluation.
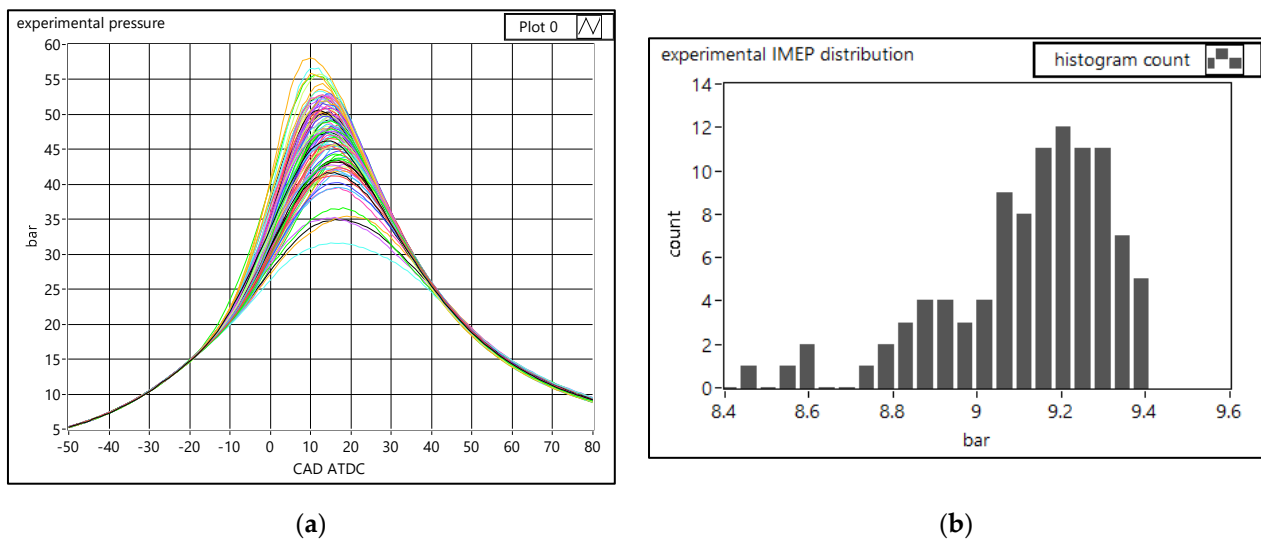

(**a**)

(**b**)

Figure 10. MAP = 1 bar, engine speed *n* = 3500 rpm, fuel 100% NG. (**a**) 100 consecutive pressure cycles; (**b**) histogram of IMEP distribution (mean value = 9.11 bar, SD = 0.214 bar).

The purpose of the procedure proposed here is to obtain, using both Wiebe and Hill functions implemented in the 0-D model described in [11], 100 simulated pressure curves with a similar IMEP distribution, i.e., the same mean value and standard deviation experimentally determined. The first step is to evaluate, from the 100 experimental pressure cycles of Figure 10a, the 100 corresponding MFB curves and, once interpolated one by one with the best matching Wiebe and Hill functions, to obtain the 100 couples of calibrating coefficients for both models. Figure 11a,b show the distribution of the 100 Hill coefficients (δ and n), which exhibit an almost Gaussian trend, while Figure 12a,b shows the distribution of the Wiebe coefficients (a and m) that once again reveal an almost Gaussian trend. Each experimental calibrating coefficient can be hence identified by a known mean value and an SD; the next step consists of the random generation of 100 couples of calibrating coefficients with a Gaussian distribution characterized by the previously determined mean value and SD. These random calibrating coefficients can be used to obtain 100 MFB curves and, in turn, 100 simulated pressure cycles. The described procedure has been carried out with both Hill and Wiebe functions to evaluate which one is more accurate in simulating the engine cyclic variation.
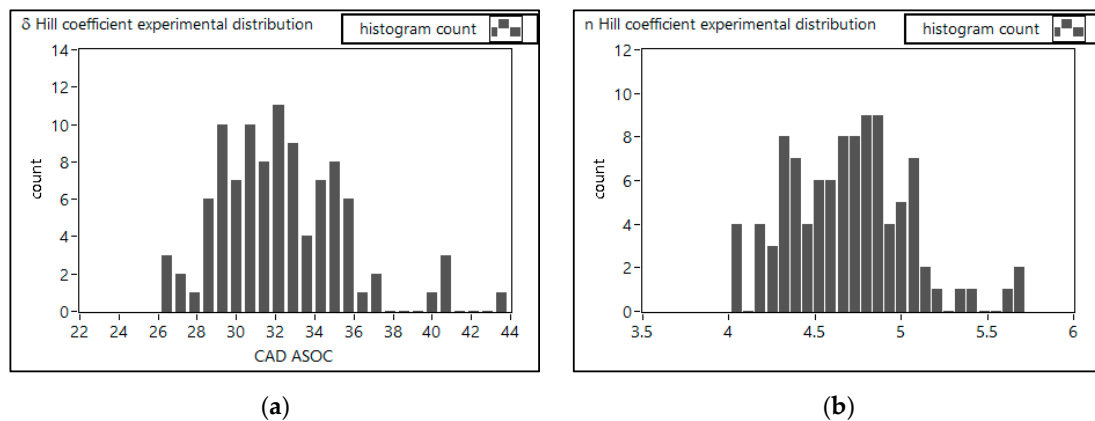
Figure 11. Histograms of Hill coefficients experimental distribution; MAP = 1 bar, n = 3500 rpm, fuel NG. (**a**) δ coefficient (mean value = 32.3 CAD, SD = 3.24 CAD; (**b**) n coefficient (mean value = 4.69, SD = 0.35).
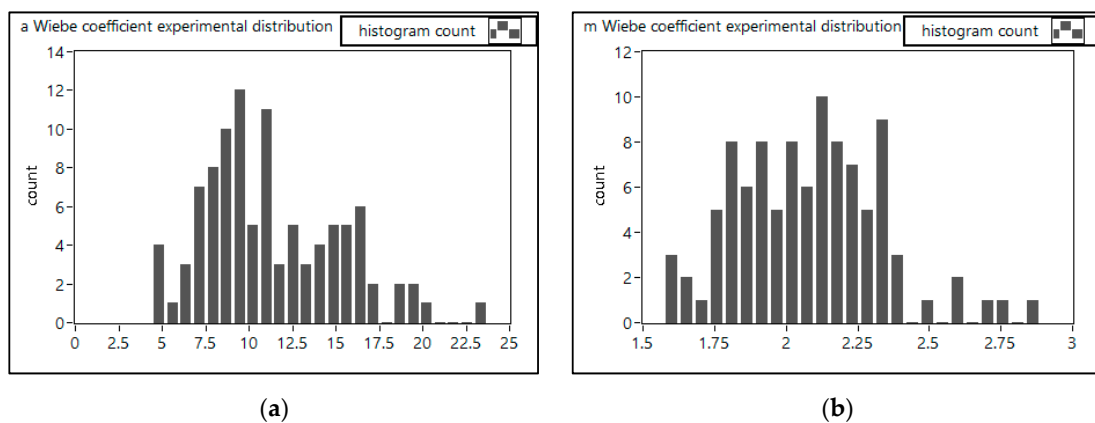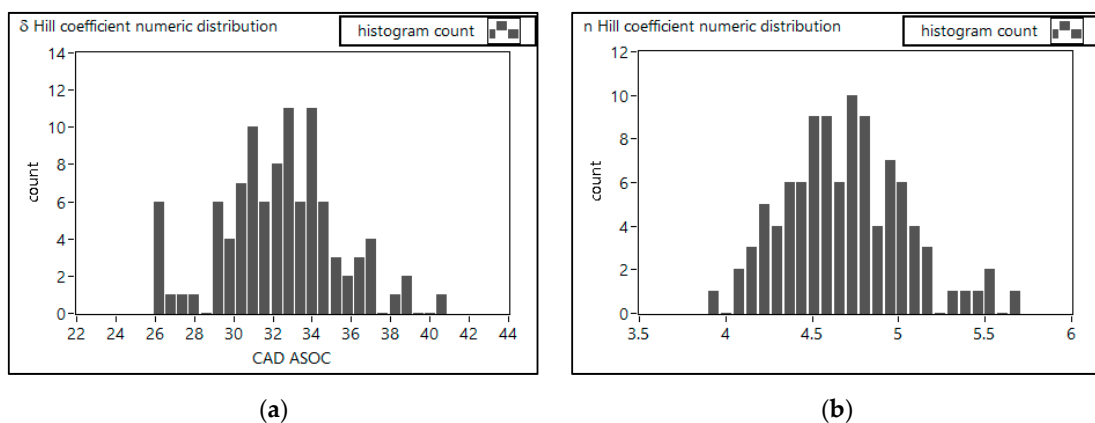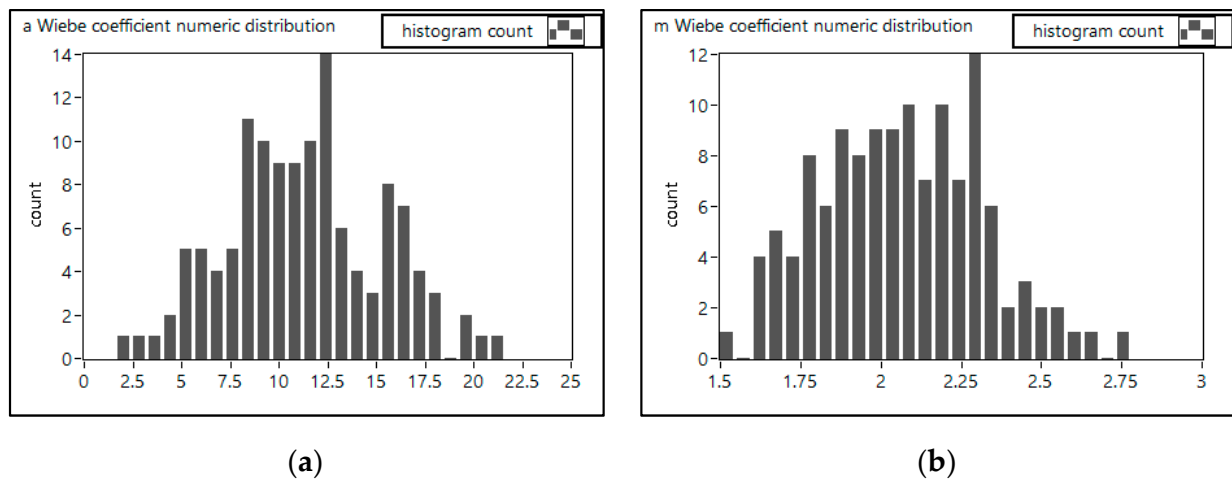

Figure 12. Histograms of Wiebe coefficients experimental distribution; MAP = 1 bar, n = 3500 rpm, fuel NG. (**a**) a coefficient (mean value = 11.2, SD = 3.93); (**b**) m coefficient (mean value = 2.08, SD = 0.254).

Figures 13 and 14 show the distributions of randomly generated calibrating coefficients; it can be noted that these distributions are quite different from the experimental ones reported in Figures 11 and 12, but the mean values and SD are the same.

Figure 13. Histograms of Hill coefficients numeric distribution; MAP = 1 bar, n = 3500 rpm, fuel NG. (**a**) δ coefficient (mean value = 32.3 CAD, SD = 3.24 CAD); (**b**) n coefficient (mean value = 4.69, SD = 0.35).

Figure 14. Histograms of Wiebe coefficients numeric distribution; MAP = 1 bar, *n* = 3500 rpm, fuel NG. (**a**) *a* coefficient (mean value = 11.2, SD = 3.93); (**b**) *m* coefficient (mean value = 2.08, SD = 0.254).

Figure 15a,b report the 100 consecutive pressure curves obtained by the 0-D simulation model described in [11] using the Hill and Wiebe equations, respectively.
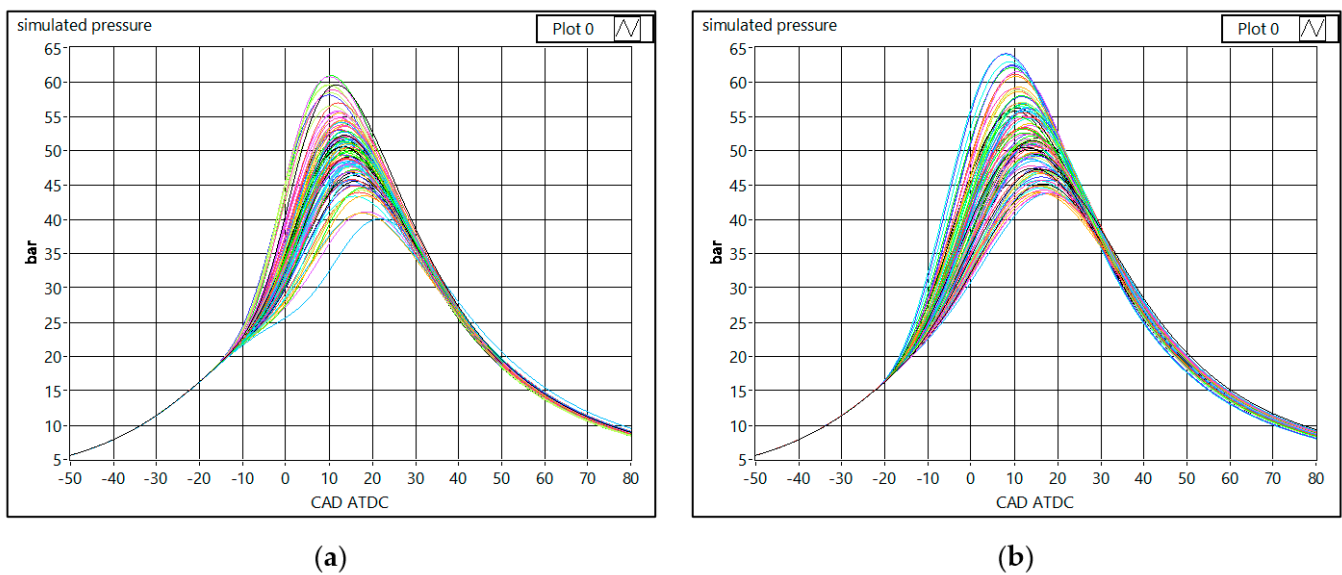

Figure 15. 100 simulated pressure cycles; MAP = 1 bar, engine speed *n* = 3500 rpm, fuel 100% NG. (**a**) using the Hill function; (**b**) using the Wiebe function.

Figure 16a,b show the numeric IMEP distribution obtained with the Hill and Wiebe equations, respectively; both the mean IMEP and SD are quite similar to the experimental values revealing an equivalent ability of both models to simulate the engine cyclic variation (the numeric results are displayed in the figures caption and resumed in Table 16).
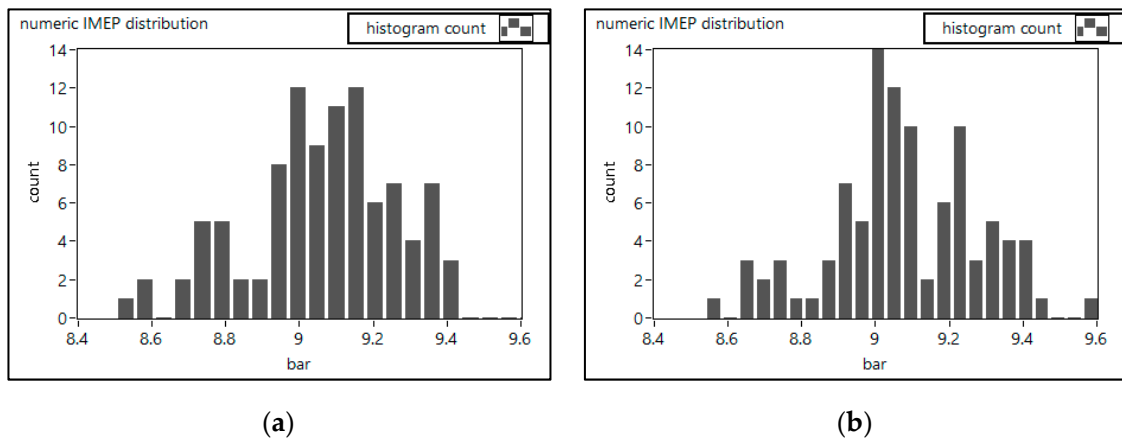
(a)   **(b)**

Figure 16. Histogram of numeric IMEP distribution; MAP = 1 bar, *n* = 3500 rpm, fuel NG. (**a**) Hill function, (mean value = 9.07 bar, SD = 0.222 bar); (**b**) Wiebe function, (mean value = 9.15 bar, SD = 0.206 bar).

Table 16. Experimental and simulated IMEP SD.

Operating Condition	Experimental IMEP SD [bar]	Simulated IMEP SD (Hill) [bar]	Error % Simulated Hill vs. Experimental	Simulated IMEP SD (Wiebe) [bar]	Error % Simulated Wiebe vs. Experimental
n = 3500 rpm MAP = 1 bar	0.214	0.222	3.74%	0.206	−3.74%
n = 2500 rpm MAP = 1.6 bar	0.239	0.236	−1.26%	0.292	22.2%

To have further confirmation, a different operating condition was explored: engine speed *n* = 2500 rpm, MAP = 1.6 bar, fuel NG. The same procedure described above was followed and two numeric IMEP distributions were determined, one using the Hill function and one using the Wiebe function. Figure 17a shows the 100 experimental pressure curves, Figure 17b reports the corresponding experimental IMEP distribution, while Figure 18a,b reports the simulated IMEP distributions obtained using the Hill and Wiebe equations, respectively.
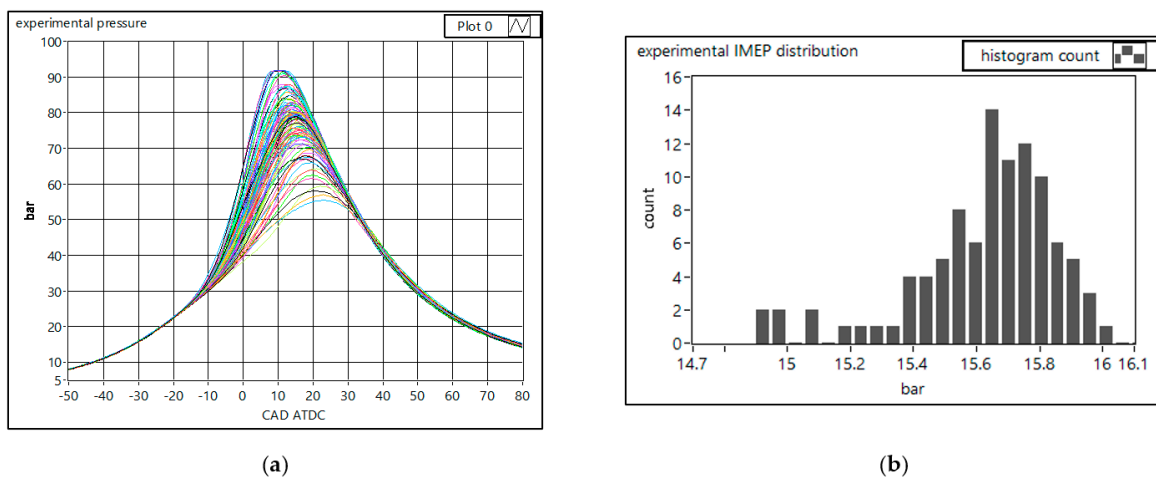

(a)   **(b)**

Figure 17. MAP = 1.6 bar, engine speed *n* = 2500 rpm, fuel 100% NG. (**a**) 100 consecutive pressure cycles; (**b**) histogram of IMEP distribution (mean value = 15.6 bar, SD = 0.239 bar).
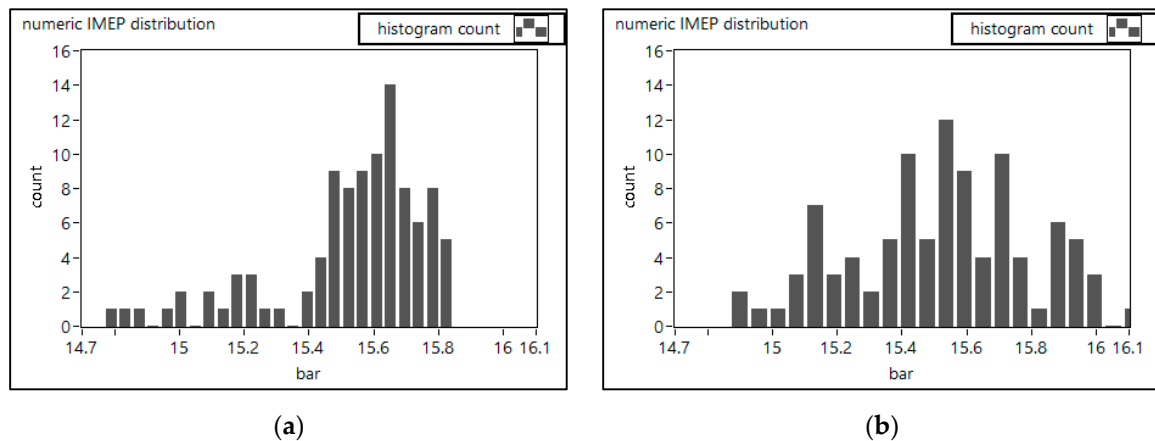
Figure 18. Histogram of numeric IMEP distribution; MAP = 1.6 bar, *n* = 2500 rpm, fuel NG. (**a**) Hill function, (mean value = 15.5 bar, SD = 0.236 bar); (**b**) Wiebe function, (mean value = 15.5 bar, SD = 0.292 bar).

In this operating condition, the Hill function predicted more accurately the pressure cyclic variation, as can be seen by comparing the two numeric IMEP distributions and, in particular, observing the IMEP SD values resumed in Table 16: considering the two operating conditions, the Hill function predicts the IMEP SD with a maximum error of 3.74% respect to the experimental values while the Wiebe function exhibit a maximum prediction error of 22.2%. Hence it can be concluded that both Wiebe and Hill functions allow to correctly predict the pressure cyclic variation of the engine by simply imposing a random variation of the calibrating coefficients with a Gaussian distribution around the mean values and the Hill function reveals more accuracy.

4. Conclusions

This work further develops previous research by the same authors [11], in which the Hill function has been proposed as a valid alternative to the classic Wiebe function to simulate the MFB curve in an NG fueled supercharged SI engine and to predict the engine IMEP correctly. In the present paper, the same supercharged engine has been fueled with mixtures of gasoline and NG in different proportions and with different supercharging pressures allowing to obtain a wider variety of operating conditions. The Hill function provided a more accurate IMEP prediction compared to the Wiebe function in all the tested operating conditions, with a maximum prediction error of 2.7% compared to 4.3% of the Wiebe function. This allows extending the validity of the Hill function to fuel mixtures composed of gasoline and NG in any proportion. The better IMEP prediction is due to the better experimental MFB curve interpolation of the Hill function (see Figure 1). In this paper, it has also been tested the ability of both Hill and Wiebe equations to predict the pressure cyclic variation of the SI engine; the IMEP SD has been identified as the cyclic variation intensity indicator, and, once again, the Hill function revealed more accuracy compared to the Wiebe function in predicting the IMEP SD with a maximum error of 3.74% with respect to 22.2% of the Wiebe function. The higher IMEP SD prediction accuracy is probably due to the higher sensitivity of the Hill function to the variation of the calibration coefficients with respect to the Wiebe function.

Institutional Review Board Statement: Not applicable.

Informed Consent Statement: Not applicable.

Data Availability Statement: Not applicable.

Conflicts of Interest: The authors declare no conflict of interest.

References

1. Matthias, N.S.; Wallner, T.; Scarcelli, R. Analysis of Cyclic Variability and the Effect of Dilute Combustion in a Gasoline Direct Injection Engine. *SAE Int. J. Engines* **2014**, *7*, 633–641. [CrossRef]
2. Baêta, J.G.C.; Pontoppidan, M.; Silva, T. Exploring the limits of a down-sized ethanol direct injection spark ignited engine in different configurations in order to replace high-displacement gasoline engines. *Energy Convers. Manag.* **2015**, *105*, 858–871. [CrossRef]
3. Millo, F.; Perazzo, A.; Pautasso, E. Optimizing the Calibration of a Turbocharged GDI Engine through Numerical Simulation and Direct Optimization. *SAE Int. J. Engines* **2010**, *3*, 556–570. [CrossRef]
4. Lecointe, B.; Monnier, G. Downsizing a Gasoline Engine Using Turbocharging with Direct Injection. *SAE* **2003**, SAE Paper 2003-01-0542. [CrossRef]
5. D'Ambrosio, S.; Spessa, E.; Vassallo, A.; Ferrera, M.; Peletto, C. Experimental Investigation of Fuel Consumption, Exhaust Emissions and Heat Release of a Small-Displacement Turbocharged CNG Engine. *SAE* **2006**, SAE Paper 2006-01-0049. [CrossRef]
6. Lake, T.; Stokes, J.; Murphy, R.; Osborne, R.; Schamel, A. Turbocharging Concepts for Downsized DI Gasoline Engines. *SAE* **2004**, SAE Paper 2004-01-0036. [CrossRef]
7. Pipitone, E.; Beccari, S. Performances improvement of a S.I. CNG bi-fuel engine by means of Double-Fuel injection. *SAE* **2009**, SAE Paper 2009-24-0058. [CrossRef]
8. Pipitone, E.; Beccari, S. Performances and Emissions Improvement of an S.I. Engine Fuelled by LPG/Gasoline Mixtures. *SAE* **2010**, SAE Technical Paper 2010-01-0615. [CrossRef]
9. Pipitone, E.; Beccari, S.; Genchi, G. Supercharging the Double-Fueled Spark Ignition Engine: Performance and Efficiency. *J. Eng. Gas Turbines Power* **2017**, *139*, 102809. [CrossRef]
10. Beccari, S.; Pipitone, E. Detailed Combustion Analysis of a Supercharged Double-Fueled Spark Ignition Engine. *SAE Int. J. Engines* **2021**, *15*, 2022. [CrossRef]
11. Beccari, S.; Pipitone, E. An Effective Method to Model the Combustion Process in Spark Ignition Engines. *SAE Int. J. Engines* **2022**, *16*, 2023. [CrossRef]
12. Heywood, J.B. *Internal Combustion Engine Fundamentals*; McGraw-Hill: New York, NY, USA, 1988.
13. Ferguson, C.; Kirkpatrick, A. *Internal Combustion Engines: Applied Thermosciences*; John Wiley & Sons, Inc.: Hoboken, NJ, USA, 2016.
14. Onorati, A.; Montenegro, G. *1D and Multi-D Modeling Techniques for IC Engine Simulation*; SAE International: Warrendale, PA, USA, 2020; ISBN 978-0-7680-9352-0.
15. Heywood, J.B. Engine combustion modeling—An overview. In *Combustion Modeling in Reciprocating Engines*; Mattavi, J.N., Amann, C.A., Eds.; Plenum Press: New York, NY, USA, 1978; pp. 1–35.
16. Blizard, N.C.; Keck, J.C. Experimental and Theoretical Investigation of Turbulent Burning Model for Internal Combustion Engines. *SAE* **1974**, SAE Technical Paper 740191. [CrossRef]
17. Keck, J.C.; Heywood, J.B.; Noske, G. Early Flame Development and Burning Rates in Spark Ignition Engines and Their Cyclic Variability. *SAE* **1987**, SAE Technical Paper 870164. [CrossRef]
18. Tabaczynski, R.J.; Ferguson, C.R.; Radhakrishnan, K. A Turbulent Entrainment Model for Spark-Ignition Engine Combustion. *SAE* **1977**, SAE Technical Paper 770647. [CrossRef]
19. Wiebe, I.I. Semi-empirical expression for combustion rate in engines. In *Proceedings of Conference on Piston engines, USSR*; Academy of Sciences: Moscow, Russia, 1956; pp. 185–191.
20. Alam, S.S.; Rosa, S.W.; Depcik, C.; Burugupally, S.P.; McDaniel, E.; Hobeck, J.D. Modification of the Wiebe function for methane-air and oxy-methane- based spark-ignition engines. *Fuel* **2021**, *303*, 121218. [CrossRef]
21. Ghojel, J.I. Review of the development and applications of the Wiebe function: A tribute to the contribution of Ivan Wiebe to engine research. *Int. J. Engine Res.* **2010**, *11*, 297–312. [CrossRef]
22. Zhou, Y.C.; Hariharan, D.; Yang, R.N.; Mamalis, S.; Lawler, B. A predictive 0-D HCCI combustion model for ethanol, natural gas, gasoline, and primary reference fuel blends. *Fuel* **2019**, *237*, 658–675. [CrossRef]
23. Yeliana, Y.; Cooney, C.; Worm, J.; Michalek, D.; Naber, J. Estimation of double-Wiebe function parameters using least square method for burn durations of ethanol-gasoline blends in spark ignition engine over variable compression ratios and EGR levels. *Appl. Therm. Eng.* **2011**, *31*, 2213–2220. [CrossRef]
24. Brehob, D.D.; Newman, C.E. Monte Carlo Simulation of Cycle by Cycle Variability. *SAE* **1992**, SAE Technical Paper 922165. [CrossRef]